(%)

	1993	1994	1997	1998	1999	2000	2005-2007	2009
Paraben mix	1.8	1.5	1.1	1.3	1.3	1.7	1.0	2.5
Formaldehyde	1.2	2.6	2.4	4.0	3.6	1.6	1.3	2.0
Kathon CG	1.3	1.5	0.9	1.6	1.1	0.9	1.0	1.2
Thimerosal	4.7	5.8	4.7	5.6	4.6	4.8	4.0	2.9

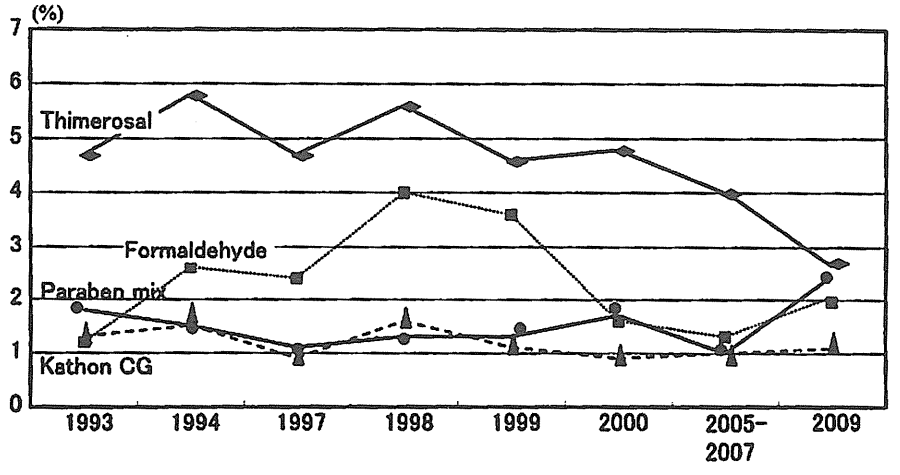

Fig. 10 : Annual variations of positive rates of preservative allergens

(%)

	1993	1994	1997	1998	1999	2000	2005-2007	2009
Urushiol	9.3	10.4	8.8	8.5	9.8	9.8	6.4	10.3
Primin	0.7	0.6	0.6	0.8	1.0	1.0	0.7	0.8
Sesquiterpene lactone mix	n.d.	n.d.	n.d.	n.d.	n.d.	n.d.	n.d.	1.5

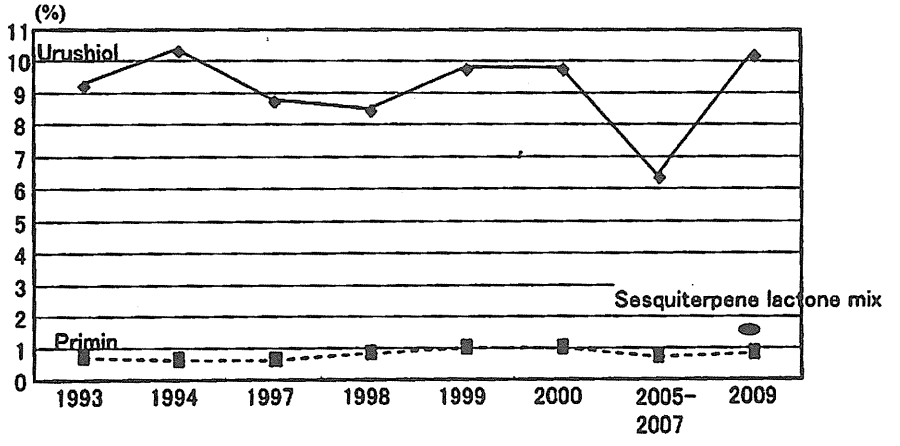

Fig. 11 : Annual variations of positive rates of plant allergens

sesquiterpene lactone mix の 2009 年度陽性率は 1.5%であった。

7）合成樹脂関連アレルゲン (Fig. 12)

陽性率に特に変化はない結果であった。ジャパニーズスタンダードアレルゲン (2008) で新たに追加された epoxy resin の 2009 年度陽性率は 0.9%であった。

考　案

1994 年に日本接触皮膚炎学会で決定された標準

(%)

	1993	1994	1997	1998	1999	2000	2005-2007	2009
Rosin	2.3	2.2	1.7	2.3	2.0	2.2	2.1	2.3
p-tertiary-Butylphenol formaledehyde resin	1.7	1.3	1.2	1.5	1.9	2.2	1.6	1.5
Epoxy resin	n.d.	n.d.	n.d.	n.d.	n.d.	n.d.	n.d.	0.9

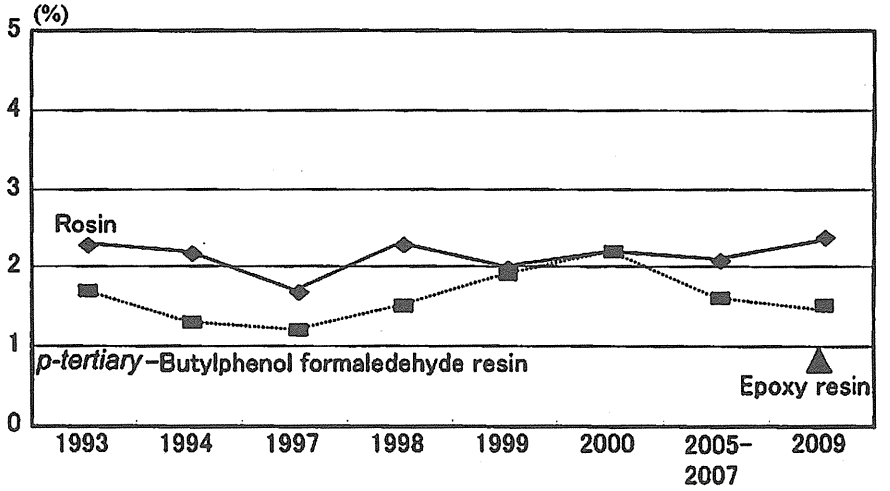

Fig. 12：Annual variations of positive rates of synthetic resin allergens

アレルゲン（Table 1）のうち，bisphenol A は環境ホルモンの問題から 2001 年より欠番として貼布しておらず，今回の見直しでは削除することとし，その代わりに欧米のスタンダードアレルゲンシリーズに加わっている epoxy resin を合成樹脂のアレルゲンとして加えることとした。また，ethylene diamine 2HCL はその陽性率が低く推移し，スタンダードアレルゲンとして適当ではないと判断し，外すこととした。一方で，gold sodium thiosulfate はピアス装着率の増加による金皮膚炎症例の増加という社会的背景を受けて，1995 年，1998 年，1999 年，2000 年に標準アレルゲンに追加して貼布し，その陽性率を検討したが，いずれも高い陽性率であったことからジャパニーズスタンダードアレルゲン 2008 に追加された。さらに日本人に多い職業性接触皮膚炎の原因物質の 1 つである菊のアレルゲンである sesquiterpene lactone mix を追加し，ジャパニーズスタンダードアレルゲン 2008 とした。

前述したように，学会からのアレルゲン配布が困難であるため，ジャパニーズスタンダード（2008）は市販されている Brial allergen と鳥居薬品株式会社パッチテスト試薬から構成されている。したがって，これまでの陽性率と 2009 年度ジャパニーズスタンダードアレルゲン（2008）の陽性率は一概に比較検討することはむずかしく，今後もジャパニーズスタンダードアレルゲン（2008）の陽性率の推移を検討していく必要がある。

特に金アレルゲンである gold sodium thiosulfate については，伊佐見ら[7]が Brial allergen の gold sodium thiosulfate（0.25%pet, 0.5%pet）と TROLAB allergen の gold sodium thiosulfate（0.25%pet）を同時に貼布してその陽性率を検討して報告している。その結果，学会が推奨している Brial allergen gold sodium thiosulfate 0.5%pet よりも TROLAB allergen gold sodium thiosulfate 0.25%pet のほうが陽性率が高い結果であった（Table 9）。このことを踏まえ，本学会としてはしばらく gold sodium thiosulfate のパッチテストアレルゲンとしては TROLAB allergen の gold sodium thiosulfate 0.25%pet を推奨することとした。この両アレルゲンの陽性率の差をもたらした要因については現在調査中であるが金チオ硫酸ナトリウムをワセリンに分散する際の技術的な要因が推測されている。

水銀はジャパニーズスタンダードアレルゲン（2008）で使用している鳥居パッチテスト試薬の塩化第二水銀（0.05% aq）とジャパニーズスタンダードアレルゲン（1994）で使用していた学会配布

Table 9 : Positive rates of 0.5%pet and 0.25% pet gold sodium thiosulfate from Brial allegens and 0.25%pet gold sodium thiosulfate from TROLAB allergens

	Brial (0.5%pet)		Trolab (0.25%pet)		Brial (0.25%pet)	
	72hrs	Day 7	72hrs	Day 7	72hrs	Day7
1	+	+	+	+	+	+
2	+	+	+	+	+	+
3	−	+	+	+	+	+
4	−	−	+	+	+?	+
5	−	−	+	+	+	+
6	−	−	+	+	+	+
7	+	+	+	+	−	−
8	+?	+	+?	+	−	−
9	−	−	+	+	−	−
10	−	−	+	+	−	−
11	−	−	+	+	−	−
12	−	−	+	+	−	−
14	−	−	+	+	−	−
16	−	−	+	+	−	−
17	−	−	+	+	−	−
18	−	−	−	+	−	−
19	−	−	−	+	−	−
20	−	−	−	+	−	−
21	−	−	+	+	−	−
22	−	−	+	+	−	−
23	−	−	+	+	−	−
24	−	−	+	+	+	+
25	−	−	+?	+	−	−
13	−	−	−	−	−	+
15	−	−	−	−	+	+?

Positive rates of three gold allergens

Brial 0.5% pet. allergen : 20.0% (5cases/25cases)

Brial 0.25%pet.allergen : 36.0% (9cases/25cases)

TROLAB 0.25%pet. allergen : 92.0% (23cases/25cases)

(ICDRG)

の塩化第二水銀（0.1%pet）とは濃度も基剤も異なっているためその陽性率の推移は基剤と濃度に留意する必要がある。このように金属アレルゲンの陽性率の低下が本当に金属感作例の減少を反映しているのか否かという点については今後数年の集計による推移を待たねばならない。

Fradiomycin sulfate の陽性率は前回の集計と同じ程度の陽性率であり，その理由としてアレルギー性結膜炎による眼周囲皮膚炎に対する fradiomycin sulfate 含有眼軟膏の使用頻度の増加が考えられる。

ジャパニーズスタンダードアレルゲン（2008）については，水銀以外のアレルゲンではこれまでのジャパニーズスタンダードアレルゲン（1994）と同じ濃度・基剤のアレルゲンを用いているが，gold sodium thiosulfate の検討で認められたように，調整方法が異なるための陽性率の変化という点に留意しなくてはならず，日本人における感作例の増減については今後のデータの蓄積が必要である。

文　献

1) Adachi A : Results of patch test with standard allergen series of the Research Group of the Japanese Society for Contact Dermatitis in 1994 and annual variations of patients with pigmented contact dermatitis of lichenoid type in 1993. Environ Dermatol. 3 : 140-150, 1996

2) Miyoshi H : Large-scale patch-testing with Japanese standard series, gold sodium thiosulfate, thimerosal, and mercuric chloride, and the number of new patients with pigmented contact dermatitis in 1994. Environ Dermatol. 4 : 95-103, 1997

3) Mitsuya K：A multicenter survey of patch-testing with Japanese standard series, topical steroid preparations (budesonide, amcinonide and hydrocortisone butylate) and tin chloride (0.5%, 1.0% and 2.0% pet) in 1997, Environ Dermatol, 6：199-208, 1999
4) Natsuaki M：Results of patch testing with standard allergens of the Japanese Society for Contact Dermatitis and topical nonsteroidal anti-inflammatory preparations in 1998, Environ Dermatol, 7：1-5, 2000
5) Sugiura M：Group study with standard allergen series of the Japanese Society for Contact Dermatitis and gold sodium thiosulfate by patch testing in 1999, Environ Dermatol, 9：105-115, 2002
6) Kurikawa Y：Group study of the optimum concentrations of ketoprofen, tiaprofenic acid, suprofen and oxybenzone for the photopatch testing, and the patch test results of the Japanese Standard Allergens and gold sodium thiosulfate in 2000, Environ Dermatol, 9：39-46, 2002
7) 伊佐見真実子, 矢上晶子, 古田加奈子他：金属の貼布材料による陽性率の比較検討, アレルギー, 59：1461, 2010

Allergic contact dermatitis caused by a skin-lightening agent, 5,5′-dipropylbiphenyl-2,2′-diol

Kayoko Suzuki[1], Akiko Yagami[2] and Kayoko Matsunaga[2]

[1]*Department of Dermatology, Kariya Toyota General Hospital, 5-15, Sumiyoshi-cho, Kariya 448-8505, Japan and* [2]*Department of Dermatology, Fujita Health University School of Medicine, 1-98, Dengakugakubo, Kutsukake-cho, Toyoake 470-1192, Japan*

doi: 10.1111/j.1600-0536.2011.01986.x

Key words: allergic contact dermatitis; cosmetics; 5,5′-dipropylbiphenyl-2,2′-diol; skin-lightening agent.

Many skin-lightening agents are currently available, including kojic acid, arbutin, hydroquinone, and 5,5′-dipropylbiphenyl-2,2′-diol (Fig. 1); the last of these is a relatively new skin-lightening agent that has been used in Japanese cosmetics since 2006. 5,5′-Dipropylbiphenyl-2,2′-diol is a biphenyl derivative, and downregulates melanin synthesis by inhibiting tyrosinase maturation, leading to accelerated tyrosinase degradation (1). Here, we report a case of allergic contact dermatitis caused by 5,5′-dipropylbiphenyl-2,2′-diol.

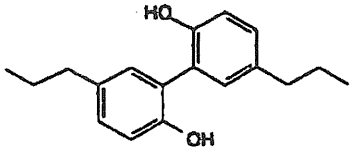

Molecular formula: $C_{18}H_{22}O_2$

Molecular weight: 270.372

CAS number: 20601-858-8

Fig. 1. Chemical formula of 5,5′-dipropylbiphenyl-2,2′-diol.

Case Report

A 45-year-old female presented with a 2-month history of an itchy erythematous rash on her cheek and neck. She had a negative history for dermatitis. Previously, she had been instructed to apply 0.3% prednisolone valerate acetate ointment twice daily by another dermatologist, but as cosmetic dermatitis was not suspected at the time, she had continued to use her cosmetics, with gradual worsening of the symptoms. We treated her with a regimen of oral prednisolone 20 mg daily for 4 days, olopatadine hydrochloride 10 mg daily for 1 week, and 0.1% hydrocortisone butyrate ointment, and advised her to stop using her cosmetics; her symptoms subsequently improved. Patch tests were performed with her personal cosmetics and 17 cosmetic allergens, using Finn Chambers® on Scanpor® tape. Readings were performed on D2 and D4 according to the International Contact Dermatitis Research Group guidelines. The patient showed positive reactions to a cream (+ on D2 and D4) and beauty essence (+ on D2 and D4), both of which were started 2 months prior to appearance of the rash. In the second patch test, with cosmetic ingredients provided by the cosmetic supplier, she reacted only to 5,5′-dipropylbiphenyl-2,2′-diol (0.5% pet., + on D2 and D4), which was present in both the cream and the beauty essence as a skin-lightening agent. The skin did not lighten over the area of the patch test with this chemical. Other cosmetic ingredients and cosmetic allergens gave negative reactions. Patch tests with 5,5′-dipropylbiphenyl-2,2′-diol 0.5% pet. in 4 control subjects gave negative results.

Discussion

Cosmetics with skin-lightening agents are popular in Japan. Cosmetics containing skin-lightening agents such as arbutin (2), hydroquinone and kojic acid have been reported to cause allergic contact dermatitis. 5,5′-Dipropylbiphenyl-2,2′-diol, an inhibitor of melanin synthesis synthesized by an oxidative coupling method (3), is a relatively new skin-lightening agent that has been marketed in Japan since 2006. Initial studies on this agent did not find adverse skin reactions. A double-blind test

Correspondence Kayoko Suzuki, Department of Dermatology, Kariya Toyota General Hospital, 5-15 Sumiyoshi-cho, Kariya 448-8505, Japan
Tel: +81-566-21-2450, Fax: +81-566-22-2493 E-mail: kayokos@fujita-hu.ac.jp

Conflicts of interest The authors have declared no conflicts of interest

was conducted on 43 subjects to determine the efficacy of formulations containing 0.5% 5,5′-dipropylbiphenyl-2,2′-diol for the treatment of ultraviolet (UV)-induced pigmentation, and showed a significant difference in pigmentation score from placebo, with no adverse skin reactions (4). The skin-lightening effects of 6 months of application of 0.5% 5,5′-dipropylbiphenyl-2,2′-diol for facial hyperpigmentation were studied in 51 Japanese females, and no adverse effects were recorded (5). Another study investigating its effect on UV-induced facial skin hyperpigmentation in 300 Japanese females did not report adverse effects after application for 1 month (6).

The first case of allergic contact dermatitis caused by 5,5′-dipropylbiphenyl-2,2′-diol was described in 2009 (7). This first case reacted positively to 5,5′-dipropylbiphenyl-2,2′-diol 1% pet. In the present case, patch testing was performed with 5,5′-dipropylbiphenyl-2,2′-diol 0.5% pet., as the amount of 5,5′-dipropylbiphenyl-2,2′-diol permitted for use in cosmetics is less than 0.5%.

This case highlights the possibility of allergic contact dermatitis caused by skin-lightening agents in cosmetics. Determination of the optimum patch test concentration of 5,5′-dipropylbiphenyl-2,2′-diol may be required in further cases of allergic contact sensitivity caused by this agent.

References

1 Nakamura K, Yoshida M, Uchiwa H, Kawa Y, Mizoguchi M. Down-regulation of melanin synthesis by a biphenyl derivative and its mechanism. *Pigment Cell Res* 2003; 16: 494–500.

2 Sugawara K, Kobayashi H, Terazawa K, Ishii M, Kato A. A case of contact dermatitis due to arbutin. *Environ Dermatol* 2002; 9: 146–148 (in Japanese).

3 Sartori G, Maggi R, Bigi F, Arienti A, Casnati G. Oxidative coupling of dichloroaluminium phenolates: highly selective synthesis of hydroxylated bi- and terphenyls. *Tetrahedron* 1992; 48: 9483–9494.

4 Takeda K, Yokota T, Ikemoto T, Kakishima H, Matsuo T. Inhibitory effect of a formulation containing 0.5% magnolignan (5,5′-dipropylbiphenyl-2,2′-diol) on UV-induced skin pigmentation. *Nishinihon J Dermatol* 2003; 65: 288–292 (in Japanese).

5 Takeda K, Arase S, Sagawa Y, et al. Clinical evaluation of the topical application of magnolignan (5,5′-dipropyl-biphenyl-2,2′-diol) for hyperpigmentation on the face. *Nishinihon J Dermatol* 2003; 65: 293–298 (in Japanese).

6 Yokota T, Sasaki M. Development of whitening cosmetics with Magnolignan on inhibitory effect of the maturation of tyrosinase. *Fragr J* 2003; 34: 80–83 (in Japanese).

7 Tsuruta K, Inaba Y, Nakagawa M, Matsunaga K. Allergic contact dermatitis from 5,5′-dipropylbiphenyl-2,2′-diol. *J Environ Dermatol Cutan Allergol* 2009; 3: 168 (oral presentation abstract, in Japanese).

Measurement of Skin Permeation/Penetration of Nanoparticles for Their Safety Evaluation

Eriko Kimura,[a] Yuichiro Kawano,[a] Hiroaki Todo,[a] Yoshiaki Ikarashi,[b] and Kenji Sugibayashi*[,a,c]

[a] *Faculty of Pharmaceutical Sciences, Josai University;* [c] *Life Science Research Center, Josai University; 1–1 Keyakidai, Sakado, Saitama 350–0295, Japan:* [b] *National Institute of Health Sciences; 1–18–1 Kamiyoga, Setagaya-ku, Tokyo 158–8501, Japan.* Received February 2, 2012; accepted June 5, 2012

The aim of the present study was to quantitatively evaluate the skin permeation/penetration of nanomaterials and to consider their penetration pathway through skin. Firstly, penetration/permeation of a model fluorescent nanoparticle, Fluoresbrite®, was determined through intact rat skin and several damaged skins. Fluoresbrite® permeated through only needle-punctured skin. The permeation profiles of soluble high molecular compounds, fluorescein isothiocyanate-dextrans (FITC-dextrans, FDs), with different molecular weights were also measured for comparison. The effects of molecular sizes and different skin pretreatments on the skin barrier were determined on the skin penetration/permeation of Fluoresbrite® and FDs. Fluoresbrite® was not permeated the intact skin, but FDs were permeated the skin. The skin distribution of titanium dioxide and zinc oxide nanoparticles was also observed after topical application of commercial cosmetics. Nanoparticles in sunscreen cosmetics were easily distributed into the groove and hair follicles after their topical application, but seldom migrated from the groove or follicles to viable epidermis and dermis. The obtained results suggested that nanoparticles did not permeate intact skin, but permeated pore-created skin. No or little permeation was observed for these nanomaterials through the stratum corneum.

Key words nanoparticle; titanium dioxide; skin permeation; skin penetration; damaged skin

Recently, nanotechnology has been a focus as a useful technology producing new nanometer-sized materials with new functions and properties.[1] Many nanomaterials have been developed using this technology, and various commercial products, such as medicines, foods, cosmetics and chemicals, are available on a global basis. Nanomaterials have been defined as nanometer-sized chemicals or nanometer-scaled aggregates with a one-dimensional length of 1–100 nm.[2] There are two kinds of nanomaterials: non-intentional and intentional nanomaterials. The former is exemplified by ash rising from volcanos and mountain fires as well as nanoparticles exhausted from diesel fumes, and the latter is industrial nanomaterials produced with several aims. Exposure of humans to non-intentional nanomaterials may be reduced by the progress of science and technology regarding human safety. Since many nanomaterials have been produced very rapidly, particular care should be taken regarding intensive or industrial nanomaterials, which are divided into biodegradable and non-biodegradable.[3] Liposomes, niosomes and nanosized emulsions are biodegradable nanomaterials. Toxicity may be a concern for monomers and metabolites of nanomaterials. Fullerenes and titanium dioxide (TiO_2) nanoparticles are examples of non-biodegradable nanomaterials. The toxicity and bioaccumulation of these compounds should be evaluated to confirm their safety.

Possible exposure sites of nanomaterial are the trachea, gastrointestinal tracts and skin. Cosmetics are commercial products that contain many nanomaterials, and many sunscreen cosmetics and foundations sometimes contain titanium dioxide (TiO_2) and zinc oxide (ZnO) nanoparticles. Since these cosmetics are applied daily to the skin surface, the skin penetration and safety of these nanomaterials are a concern. Wu *et al.* reported that titanium dioxide nanoparticles were migrated into other organs after permeated through the skin by continuous apply.[4] It is urgent to determine the skin penetration/permeation rate and to clarify the penetration/permeation pathway of the materials. Many reports have already suggested that these nanoparticles do not permeat the skin.[5,6] However, it is very difficult to quantitatively measure the skin permeation rate of titanium dioxide and zinc oxide nanoparticles through intact and healthy human and animal skin.[7] In addition, few reports have shown a quantitative penetration/permeation of titanium dioxide and zinc oxide nanoparticles through skin.

In the present study, Fluoresbrite® (fluorescent polystyrene latex spheres, particle size: 50 nm) was used as an easily detectable and non-dissolved model nanoparticle, and *in vitro* permeation experiments of the spheres were carried out through intact and wounded rat skin with different pretreatments. The permeation profiles of soluble high molecular compounds, fluorescein isothiocyanate-dextrans (FITC-dextrans, FDs) with different molecular weights through skin were also measured for comparison. The effects of different molecular sizes and pretreatments on the skin barrier were determined for the skin penetration/permeation of Fluoresbrite® and FDs. In addition, the skin surface distribution of titanium dioxide and zinc oxide nanoparticles was observed after topical application of commercial cosmetics.

THEORETICAL

Type of Material-Permeable Membranes Material-permeable membranes can be classed into three groups.[8] Type I is a dissolution-diffusion membrane in which materials dissolve and permeate through the membrane. A silicone membrane is an example of Type I membrane that is sometimes used as an alternative to human or animal stratum corneum. Type II is a porous membrane through which materials smaller than the pore size can permeate, for example, a dialysis membrane. Type III is a composite of dissolution-diffusion

The authors declare no conflict of interest.

* To whom correspondence should be addressed. e-mail: sugib@josai.ac.jp

and porous membranes.

Permeation through skin mainly occurs by the dissolution-diffusion phenomenon; that is, materials must dissolve in the membrane so that they can permeate the skin; however, it was reported recently that hair follicles must be an important skin permeation pathway for hydrophilic and macromolecular compounds.[9] Hair follicles are assumed to have a porous route as a Type II membrane. High molecular weight compounds and nanomaterials that are not dissolved in the skin may permeate through the hair follicular pathway.

Skin Permeability Coefficient and Desquamation Rate The permeability coefficient (P, cm/s) is a quantitative index of the skin penetration and permeation of materials. The stratum corneum generally consists of about 20 corneocyte layers with a thickness of about 20 μm. If a 1 μm corneocyte layer is desquamated from the outermost stratum corneum per day, the desquamation ratio (P_{des}) is 1.0 μm/d, that is, about 10^{-9} cm/s. If the permeability coefficient of a certain material is less than the P_{des}, material that moved through the first corneocyte layer over 24 h is not further transferred to the second layer due to desquamation of the first layer.[10] Thus, material with P less than P_{des} is not theoretically transferred to the lower layer of the stratum corneum when the dominant permeation route is through the stratum corneum. Three categories can be established by the relationship between the magnitude of P and P_{des} as follows: (i) when $P-P_{des} \gg 0$, material permeates the skin, (ii) when $P \cong P_{des}$, material penetrates the skin, and (iii) when $P-P_{des} \ll 0$, material does not permeate or penetrate the skin.

Generally, materials diffuse through and permeate the skin according to their concentration gradient though the skin barrier (stratum corneum). The skin permeation rate (dQ/dt) of material per unit area is expressed by the following Eq. (1), Fick's 1st law of diffusion in the steady state.

$$\frac{dQ}{dt} = \frac{D \cdot K \cdot C_d}{L} \quad (1)$$

In addition, the permeability coefficient (P) is expressed as follows:

$$P = \frac{D \cdot K}{L} \quad (2)$$

where D is the diffusion coefficient in the skin barrier, K is the partition coefficient between the skin barrier and vehicle, C_d is the concentration of the applied compound and L is the barrier thickness of the skin.

MATERIALS AND METHODS

Materials Fluoresbrite® yellow green plain microspheres (50 nm in average diameter) were purchased from Polyscience, Inc. (Warrington, PA, U.S.A.). FDs (FD-4, FD-20, FD-40, FD-70, FD-250, FD-2000) were purchased from Sigma Aldrich Co. (St. Louis, MO, U.S.A.). Table 1 summarizes the physicochemical properties of FDs. Sunscreen (Allie Comfortable Protector EX) was purchased from Kanebo Cosmetic Inc. (Tokyo, Japan). All other reagents and solvents were of reagent grade and used without further purification.

Animals Male hairless rats (WBN/ILA-Ht, *ca.* 200–250 g) were supplied by Life Science Research Center, Josai University (Sakado, Saitama, Japan). Porcine ear skins (LWD strain) were from Saitama Experimental Animal Laboratory (Sugito, Saitama, Japan). All animal experiments were approved by the Institutional Animal Care and Use Committee of Josai University.

***In Vitro* Skin Permeation Experiment** The skin permeation of Fluoresbrite® and FDs was assessed using excised hairless rat abdominal skin. After the rats had been anesthetized by intraperitoneal injection of sodium pentobarbital (50 mg/kg), the left and right abdominal skin was excised. The skin samples have *ca.* 0.6–0.7 mm. Stripped hairless rat skin was also used after removing the stratum corneum from the abdominal area by stripping 20 times with adhesive tape (Cellophane tape; Nichiban Co., Ltd., Tokyo, Japan). Needle-punctured skin was treated one time with a 20–30 G needle (20 G; regular-beveled, 23–27 G; short-beveled, and 30 G; used in dentistry; all from Terumo Co., Tokyo, Japan) to puncture skin to 10 mm depth from the skin surface in the effective permeation area (One pore was created in the effective permeation area.). In the preparation of needle-punctured skin, the abdominal skin was excised and set on the diffusion cell using Aron Alpha® (Toagosei Co., Ltd., Tokyo, Japan). We confirmed that the needle had completely penetrated the skin. Razor-treated skin with two wounds at 5 mm distance and 0.5 mm depth was made using a razor (Feather double-edged razor S; Feather Safety Razor Co., Ltd., Osaka, Japan) on the stratum corneum side. The depth (0.5 mm) was selected to reach the wound at top dermis and not to penetrate the cut through the excised skin. In the preparation of razor-treated skin, a razor was sandwiched between wooden chopsticks and pulled at constant pressure to make two parallel wounds at a distance of 0.5 mm in the effective permeation area. Razor-treated skin was prepared under anesthesia. Fat on the dermis side was carefully trimmed off with scissors.

These skin membranes were mounted on a side-by-side diffusion cell (effective diffusion area: 0.95 cm^2). Phosphate-buffered saline (PBS, pH 7.4) (3.0 mL) was applied to the epidermal and dermal sides and left for one hour to remove autogenic fluorescence from skin and to hydrate the stratum corneum. Skin resistance was then measured using an impedance meter (Advance, Tokyo, Japan) with Ag and AgCl electrodes at 10 Hz for the alternating current supply. After PBS had been removed from the epidermal and dermal sides, 0.26% Fluoresbrite® suspension in PBS or FDs solution in PBS (1.0 mg/mL FD-4, 1.0 mg/mL FD-20, 7.5 mg/mL FD-40, 7.5 mg/mL FD-70, and 10 mg/mL FD-250, 10 mg/mL FD-2000 on the intact skin: 1.0 mg/mL FDs on the stripped skin, razor-treated skin and needle-punctured skin) was applied to the epidermal side and 3.0 mL fresh PBS was again applied to the dermal side. The receiver solution (0.50 mL) was sampled 0 h from the dermal side compartment, and the same volume of

Table 1. Physicochemical Properties of FITC-Dextrans (FDs)

FDs	M.W. (kDa)	Stokes diameter, d (nm)	Log d (nm in d)
FD-4	3.38—4.40	2.8[11]	0.45
FD-20	21.2	6.6[11]	0.82
FD-40	35.6—38.5	9.0[11]	0.95
FD-70	69.8	12.0[11]	1.08
FD-250	250	21.0[12]	1.32
FD-2000	2000	41.6[13]	1.62

Refer to the references for the number in brackets.

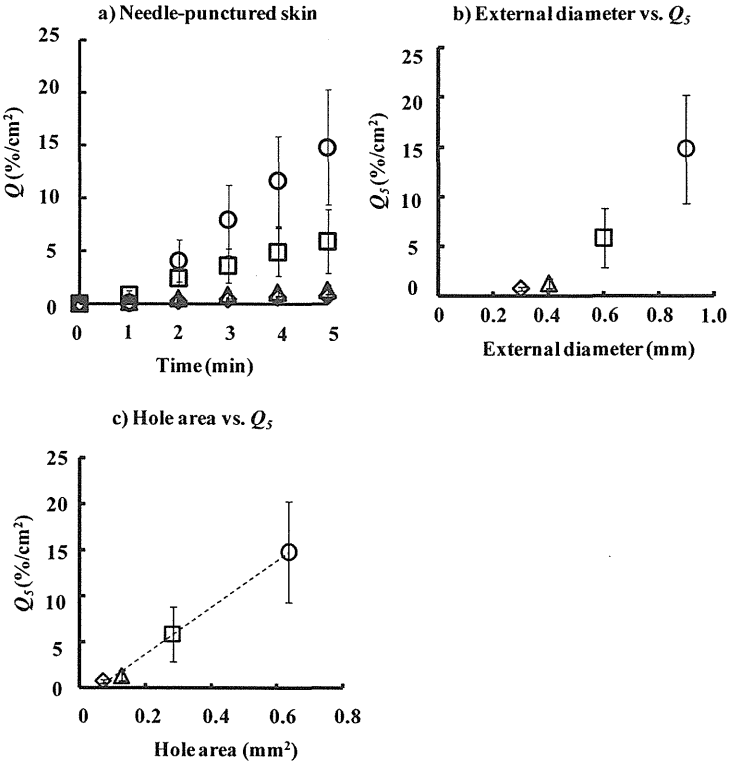

Fig. 1. Effect of Needle-Puncture on the Skin Permeation of Fluoresbrite®

a: Time course of changes in the cumulative fraction of Fluoresbrite® that permeated through needle-punctured hairless rat skin, b: relationship between external diameter and the cumulative amount of Fluoresbrite® that permeated needle-punctured skin over 5 min (Q_5), and c: relationship between pore area by needle-puncture and the cumulative amount of Fluoresbrite® that permeated through needle-punctured skin over 5 min (Q_5). Symbols: ○: 20 G needle (external diameter: 0.9 mm), □: 23 G needle (0.6 mm), △: 27 G needle (0.4 mm), ◇: 30 G needle (0.3 mm). Each point represents the mean±S.E. (n=3–4).

fresh PBS was added to continue the permeation experiments. Polysorbate 80/PBS solution (0.1%) was used to prevent air from entering the pore in the needle-punctured skin. It was confirmed that the permeation rate was not changed through other damaged skins using polysorbate 80/PBS solution. The experiment was performed at 32°C, and the epidermal and dermal sides were stirred by magnetic stirrers. Aliquots (0.50 mL) were periodically withdrawn from the dermal side compartment, and the same volume of fresh PBS was added to keep the volume constant. Fluoresbrite® or FDs concentration in each sample was determined by a fluorescence spectrophotometer (RF5300; Shimadzu, Kyoto, Japan) at excitation and emission wavelengths of 441 and 486 nm (Fluoresbrite®) or 490 nm and 520 nm (FDs).

Morphological Evaluation of Skin The skin surface of hairless rats was carefully rinsed with PBS several times to remove Fluoresbrite® attached to the skin after the permeation experiments. The skin specimens were embedded in Super Cryoembedding Medium (Leica Microsystems, Wetzlar, Germany) and frozen in isopentane at −80°C. The embedded skins were sliced using a cryostat (CM3050; Leica Microsystems, Wetzler, Germany) to obtain vertical 20 μm-thick sections. The prepared skin sections were observed with a confocal laser scanning microscope (CLSM; FV1000; Olympus Co., Tokyo, Japan).

Surface Distribution of Nanoparticles on Skin After commercial sunscreen containing titanium dioxide and zinc oxide nanoparticles had been applied to the excised porcine ear skin (2 mg/cm^2). TiO_2 and ZnO concentrations were 3.4% and 8.1%, respectively. The skin surface was observed using a scanning electron microscope (SEM, S-3400N; Hitachi High-Technologies Co., Tokyo, Japan). In addition, the skin distribution of carbon (C), titanium (Ti) and zinc (Zn) was observed using elemental mapping (EDX, X-Max50; Horiba Ltd., Kyoto, Japan). In this study, we used porcine ear skin, which is found to be similar barrier function to human skin[14–16] and have larger the hair follicles than hairless rats.

RESULTS

***In Vitro* Skin Permeation of Fluoresbrite®** Figure 1a shows the permeation profiles of Fluoresbrite® through needle-punctured skin. No permeation of Fluoresbrite® was observed not only through intact skin but also through stratum corneum-stripped skin over 24 h. In addition, interestingly, no permeation was found through the skin with deep razor wounds. On the other hand, Fluoresbrite® permeation into the receiver compartment was observed through needle-punctured skin treated by 20 to 30 G needles (Fig. 1a). A decreased G number (*i.e.* increase in needle diameter) increased the skin permeation of Fluoresbrite® (Fig. 1a). The relation between Fluoresbrite® permeation and the external diameter and cross area of the needle was evaluated, and the results are shown in Figs. 1b and c, respectively. The result in Fig. 1b is a concave upward curve. The permeation of Fluoresbrite® through needle-punctured skin was almost proportional to the pore area

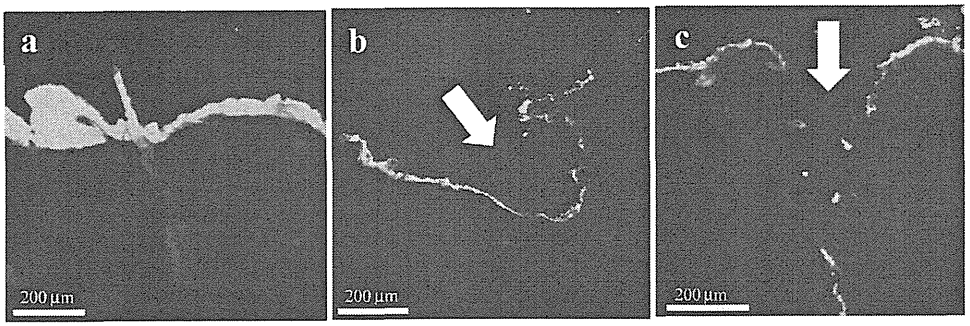

Fig. 2. CLSM Images of Vertical Slice of Hairless Rat Skin after Application of Fluoresbrite®

a: Stripped skin 24 h after application of Fluoresbrite®, b: razor-treated skin 5 min after application of Fluoresbrite®, and c: needle-punctured skin 10 min after application of Fluoresbrite®. Each bar represents 200 μm. Arrows in b and c show sites of razor-treated and needle-punctured skin, respectively.

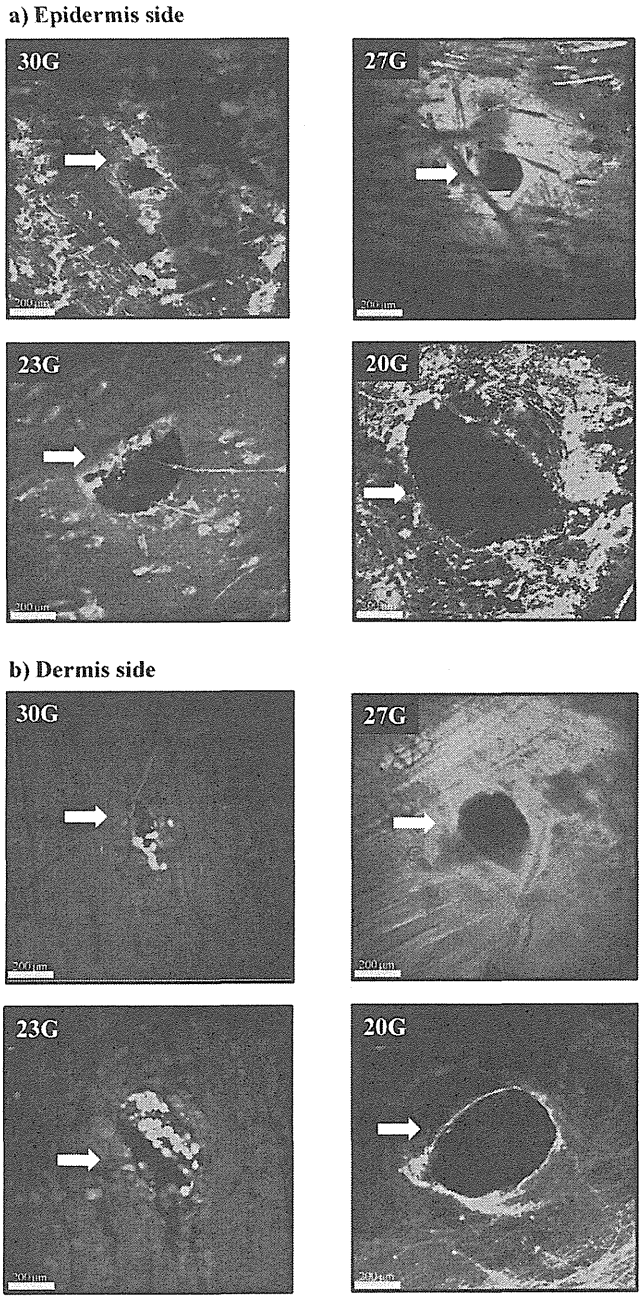

Fig. 3. CLSM Images of the Epidermis Side (a) and Dermis Side (b) of Needle-Punctured Hairless Rat Skin 5 min after Application of Fluoresbrite®

Arrows show pores created by needle puncture.

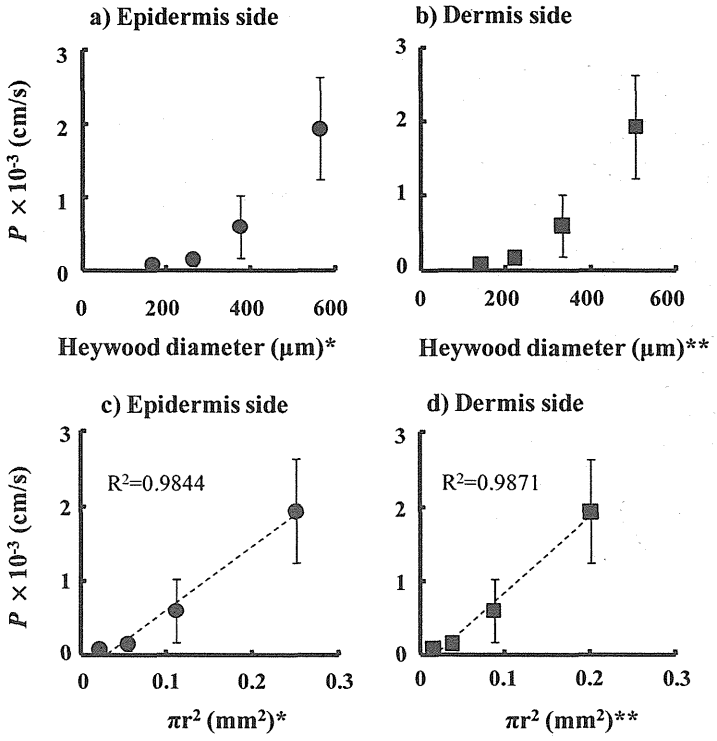

Fig. 4. Relationship between Permeability Coefficients (P) of Fluoresbrite® and Heywood Diameter (a, b) and Area (c, d) of Pores Prepared by Needle Puncture

Heywood diameter was calculated by CLSM observation from the epidermis side* and dermis side** of needle-punctured skin. The pore area was determined by $\pi\times$(Heywood diameter/2)^2. Intercepts in x-axis in Figs. 4c and d are 79 and 77 nm, respectively. The correlation coefficient was calculated by the liner regression. Each point represents the mean±S.E. (n=3).

made by the needle, as shown in Fig. 1c. The intercept of the abscissa axis was about 0.056 mm^2.

Figure 2 shows CLSM images of a vertical slice of hairless rat skin after application of Fluoresbrite®. High fluorescence was found in the skin surface 24 h after application to stripped skin (Fig. 2a). Detailed observation showed that the fluorescence was on the skin surface, not in the epidermis. Light fluorescence in the hair and around the hair follicles was probably related to autogenic fluorescence caused by hair protein. Since no fluorescence was found in the dermis, Fluoresbrite® did not permeate the viable epidermis and dermis. When Fluoresbrite® was applied to razor-treated skin, fluorescence was observed around the wound (Fig. 2b). When Fluoresbrite® was applied to needle-punctured skin, however, fluorescence was found across the pore made by the needle 10 min after application (Fig. 2c). Fluoresbrite® could permeate skin very quickly *via* the perforating pathway. The width of the fluorescence in the deep skin site was much narrower than on the skin surface.

Figures 3a and b show CLSM images of the epidermis surface (a) and dermis surface (b) of needle-punctured excised hairless rat skin 5 min after application of Fluoresbrite®. An increase in the external diameter of the needle from 30 to 20 G increased the perforating pores made by the needles. Figures 4a and b show the effect of the Heywood diameter of the pores in the epidermal and dermal surfaces, respectively, made by needles on the permeability coefficient, P, of Fluoresbrite® through the skin. The P values increased with an increase in the Heywood diameter of the pores. These figures (Figs. 4a, b) showed a concave upward curve, the same as in Fig. 1b. The relation between the P value and pore area was determined, and the results are shown in Figs. 4c and d. An almost straight line with an intercept of the abscissa axis was observed between the P value of Fluoresbrite® through the skin and pores made by needles, similar to Fig. 1c. The diameter was calculated to be about 80 μm from this intercept area. This size range may be needed for clear permeation of Fluoresbrite® of 0.05 μm (50 nm) in diameter through porous skin.

Figures 4a and b resemble Fig. 1b, and Figs. 4c and d also resemble Fig. 1c. Intercept of the abscissa axis in Fig. 1c was about 0.056 mm^2, indicating 130 μm in diameter. The difference between 130 and 80 μm suggests shrinking of the pores in the skin after pulling out the needles.

Distribution of Nanoparticles on Skin after Application of Sunscreen Figures 5 and 6 show SEM photographs of the porcine skin surface after the application of commercial sunscreen cosmetics. Figure 5 compares a wide to narrow field of view of the skin surface. Each bar in Figs. 5a, b and c is 1.0 mm, 200 μm and 50 μm, respectively. White dots indicate sunscreen. Nanoparticles in sunscreen cosmetics were easily distributed in the groove, as shown in Fig. 5b, and hair follicles, as shown in Fig. 5c, after topical application.

Figure 6 shows SEM photographs and their elemental mapping on skin after the application of sunscreen cosmetics to porcine skin. Figures 6a–f show photographs of the same site containing hair follicles. Figure 6a is the original SEM photograph. Black areas in the figure are concentrated sunscreen. Figure 6b shows the distribution of carbon (C) on the skin in

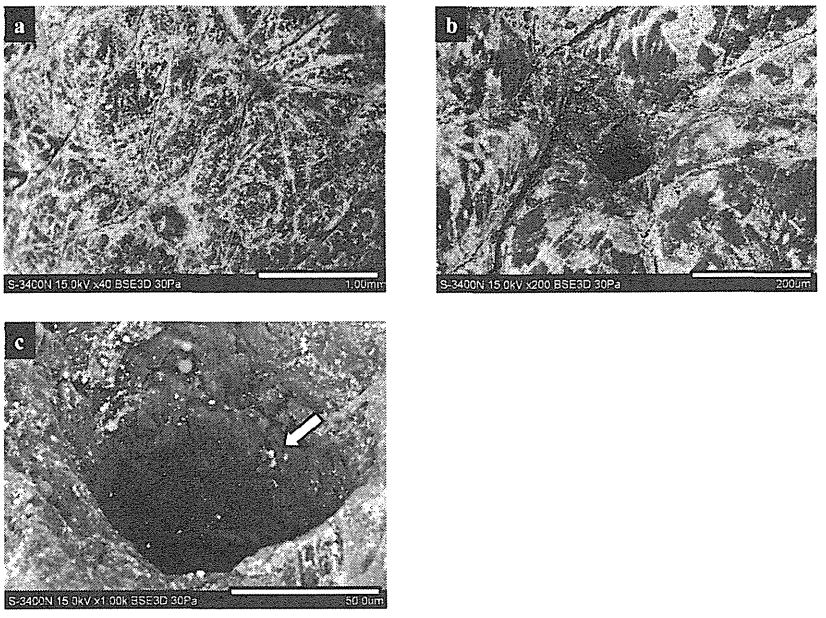

Fig. 5. SEM Images of Porcine Skin Surface after Application of Commercial Sunscreen

Arrow shows aggregated nanoparticles irrupting into hair follicles. Each white bar represents 1.0 mm (a), 200 μm (b), and 50 μm (c).

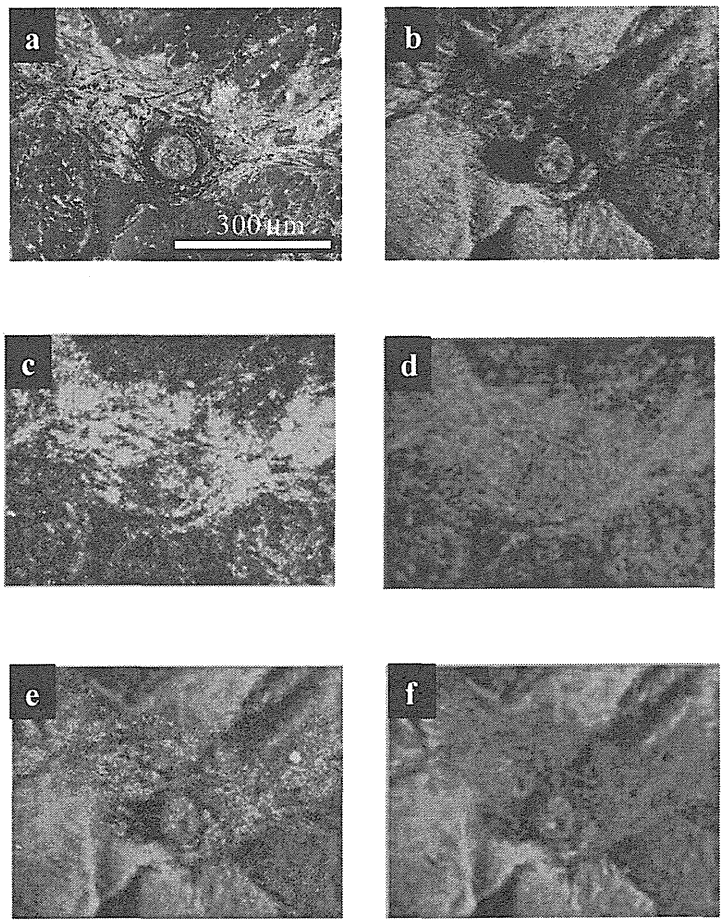

Fig. 6. SEM-EDX Elemental Mapping Images of Porcine Skin Surface after Application of Commercial Sunscreen

Original SEM image (a), carbon mapping (b), titanium mapping (c), zinc mapping (d), merged carbon and titanium mapping (e), and merged carbon and zinc mapping (f) of the same site of skin surface. A hair follicle was found almost center of the figure as clearly shown in Fig. 6a. Bar represents 300 μm.

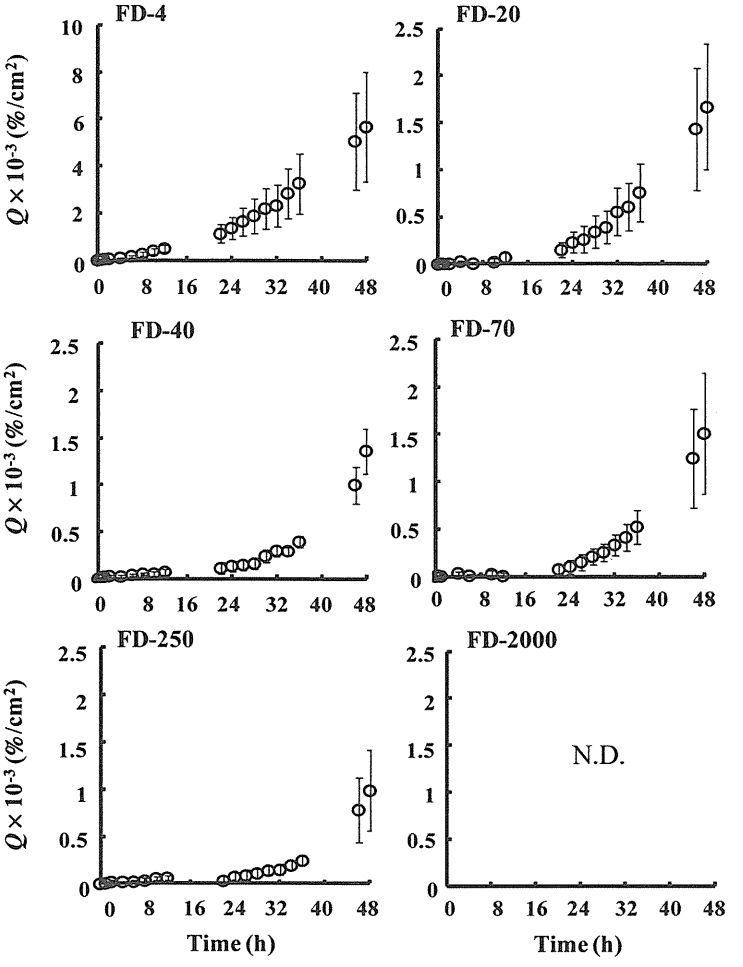

Fig. 7. Time Course of Changes in Cumulative Amount of FDs That Permeated Intact Hairless Rat Skin
Each point represents the mean±S.E. (n=3–4).

red, determined by elemental analysis. The red region is very similar to the black region in Fig. 6a, indicating low concentration of sunscreen. On the other hand, the distribution of Ti and Zn, as shown in Figs. 6c and d, respectively, is very similar, indicating a high concentration of sunscreen. In addition, these sites are very similar to the white region (high concentration of sunscreen) in Fig. 6a. Merged photographs of C+Ti and C+Zn, as shown in Figs. 6e and f, respectively, clearly suggest that titanium dioxide and zinc oxide nanoparticles are distributed in relatively deep regions, such as the groove and hair follicle infundibulum.

***In Vitro* Skin Permeation of FDs** Skin permeation of model high molecular compounds, FDs, was also determined similarly to that of Fluoresbrite®, and their permeability was compared. Figure 7 illustrates the time course of the cumulative amount of FD-4 to -2000 that permeated intact skin. FD-4 to -250 permeated intact skin, unlike the skin permeation of Fluoresbrite®. Intact skin permeability decreased with an increase in the molecular weight of FDs. A gradual increase over time was observed in the skin permeation of higher molecular weight FDs, which made it difficult to determine steady-state flux. FD-2000, with a solute diameter very similar to Fluoresbrite®, did not permeate intact skin.

Figure 8 shows the permeation of FDs through stripped skin or razor-treated skin. No change in the cumulative amount of FD-4 permeation over 8 h was observed through stripped skin and razor-treated skin, whereas higher permeation of FD-40 and FD-70 through razor-treated skin was observed than through stripped skin. The lack of difference in the permeation of FD-2000 through both types of skin may be due to low quantitative sensitivity.

Figure 9 shows a double logarithmic plot of the permeability coefficient, P, of FDs in cm/s, and the Stokes diameter, d, in nm of FDs. Log$P$ of FDs through intact skin, stripped skin and razor-treated skin had a tendency to decrease with an increase in log$d$. The reason why log$P$ of FD-70 was higher than FD-40, although there was not significant, is still unknown. Average P values for 22–36 h were used for intact skin, whereas steady-state P values were used for stripped-skin and razor-treated skin. The calculated maximum P value of FD-2000 was plotted for intact skin, since the receiver concentration was less than the quantification limit.

Figure 10 shows the effect of several treatments on the electric resistance of skin. The resistance of stripped skin was one twentieth that of intact skin. Similar data were observed for razor-treated skin. Interestingly, on the other hand, the electric resistance of needle-punctured skin was much higher than stripped skin and razor-treated skin. Fluoresbrite® only

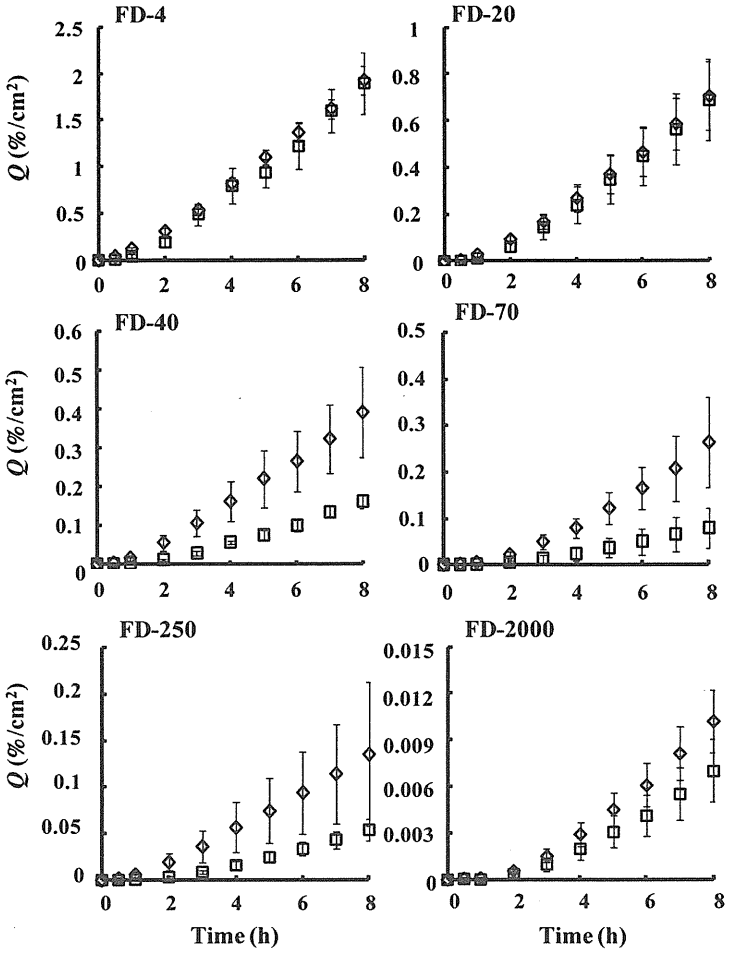

Fig. 8. Time Course of Changes in Cumulative Amount of FDs That Permeated Stripped and Razor-Treated Hairless Rat Skin

Each point represents the mean±S.E. (n=3–4).

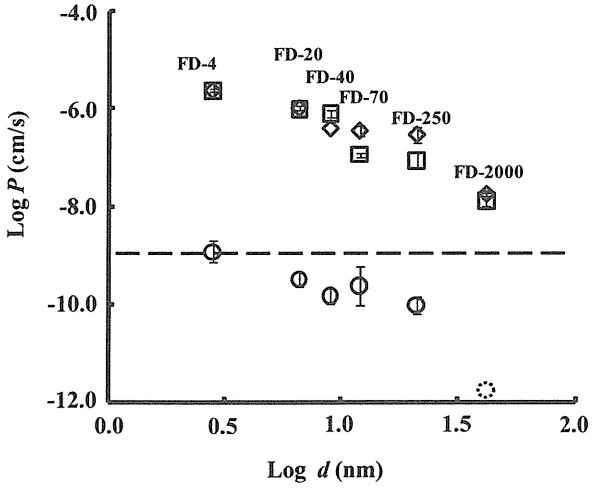

Fig. 9. Relationship between Permeability Coefficients (P) and Stokes Diameter (d) of FDs

Symbols: ○: intact skin, □: stripped skin, ◇: razor-treated skin, : FD-2000 estimated value. Dashed line shows desquamation rate. Each point represents the mean±S.E. (n=3–4).

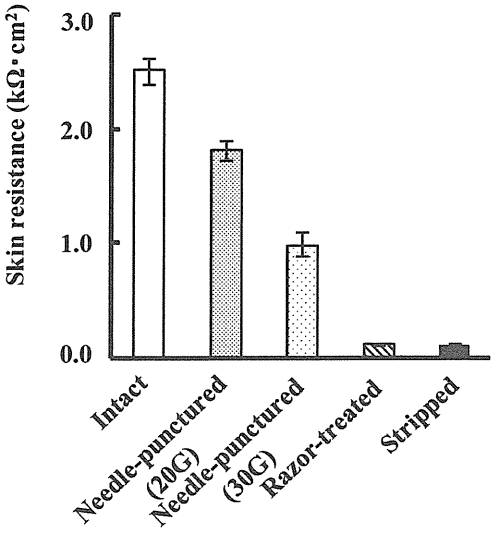

Fig. 10. Comparison of Electric Resistance in Several Hairless Rat Skin Samples 1 h after Hydration

Each value represents the mean±S.E. (n=4–5).

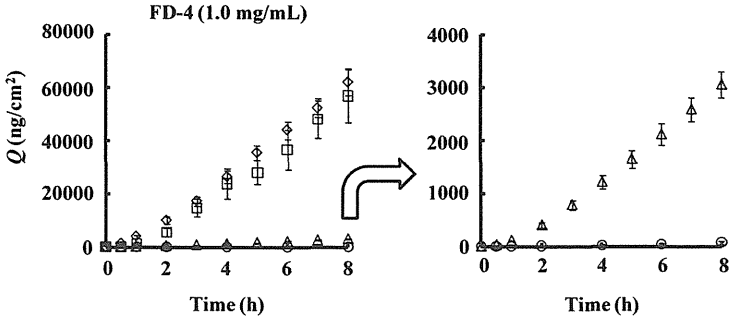

Fig. 11. Cumulative Amount in Several Skin Samples of FD-4

Symbols: ○: intact skin, □: stripped skin, ◇: razor-treated skin, △: needle-punctured skin. Each value represents the mean±S.E. (n=3–4).

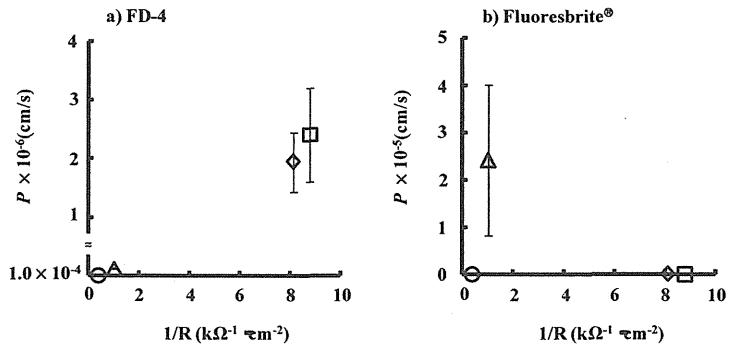

Fig. 12. Relationship between Permeability Coefficients (P) of FD-4 (a) or Fluoresbrite® (b) and Reciprocal of Electric Resistance in Several Skin Samples

Symbols: ○: intact skin, □: stripped skin, ◇: razor-treated skin, △: needle-punctured skin. Each value represents the mean±S.E. (n=3–4).

permeated needle-punctured skin, suggesting that its skin permeation was not reversely proportional to electric resistance.

Figure 11 shows the cumulative amount of FD-4 that permeated intact, stripped, razor-treated and needle-punctured skins. Unlike the skin permeation of Fluoresbrite®, FD permeation of skin increased with decreased skin resistance. Figure 12a shows the relation between the P value of FD-4 and the reciprocal of skin resistance. The figure shows that FD permeation of skin was almost proportional to the reciprocal of the electric resistance of skin. On the other hand, Fluoresbrite® permeation of skin was not dependent on skin resistance, as shown in Fig. 12b.

DISCUSSION

***In Vitro* Skin Permeation of Fluoresbrite®** Since Fluoresbrite® did not permeate intact hairless rat skin, the P value of the nanomaterial through intact skin was calculated from the quantification lower limit. The calculated P value was less than 2.4×10^{-10} cm/s. This calculated P value is less than P_{des}, as shown in the theoretical section, and must be categorized as $P-P_{des}\ll0$, suggesting that this type of nanomaterial does not permeate the greatest skin barrier, the stratum corneum. Furthermore, Fluoresbrite® did not permeate the viable epidermis and dermis, so-called stripped skin (Figs. 1a, 2a). Fluoresbrite® is not soluble in the majority of media; thus, it probably does not permeate a dissolution-diffusion membrane, a Type I membrane, explained in the theoretical section, although the nanomaterials may penetrate a cracked stratum corneum, which may be a Type II membrane (porous membrane). A CLSM image of a vertical slice of hairless rat skin (Fig. 2a) showed that the fluorescence caused by Fluoresbrite® did not permeate stripped skin. In addition, fluorescence was observed on the wound surface after topical application to razor-treated skin (Fig. 2b). On the other hand, Fluoresbrite® could permeate the perforating pores made by needles (Figs. 1a, 2c). Fluoresbrite® permeation increased with an increase in the external diameter and cross sectional area of the needle (Figs. 1b, c) and the pore size (Fig. 4), indicating that the permeability of Fluoresbrite® was closely related to the pore area. CLSM images indicated that an increase in the external diameter of the needle from 30 to 20 G increased the pore area made by the needles (Fig. 3). It was suggested from the results in Fig. 4 that about 1000-fold greater pore size may be needed for sufficient penetration of Fluoresbrite® (50 nm in diameter). Thus, Fluoresbrite® did not permeate stripped skin or razor-treated skin, but permeated needle-punctured skin. The viable epidermis and dermis layer must be a significant barrier, as well as the stratum corneum, in the overall skin permeation of Fluoresbrite®. Zhang *et al.* reported that poly(D,L-lactic-*co*-glycolic acid) (PLGA) nanosphere did not permeate the holes-formed skin produced by micro-needles.[17] They concluded that these nanoparticles were distributed into the holes. Our results with their report suggest that insoluble nanoparticles may be permeated through big pores-existing skin membrane.

Distribution of Nanoparticles on Skin after Application of Sunscreen According to SEM images of the skin surface and elementary mapping, titanium dioxide and zinc oxide

nanoparticles tended to distribute around the groove and hair follicles after application of commercial sunscreen products (Figs. 5, 6). The results suggest that these nanoparticles must accumulate in the lower level of the average skin surface.[18] Recent papers[19,20] indicated that nanoparticles do not permeate skin; however, Jeong *et al.*,[21] Lademann *et al.*[22] and Vogt *et al.*[23] reported selective penetration of nanoparticles into hair follicles.[21–24] Our present data support these results.

***In Vitro* Skin Permeation of FDs** FD-2000 with a similar solute diameter (41.6 nm) to Fluoresbrite® (50 nm) did not permeate intact skin (Fig. 7). This difference in the skin permeation of FD-2000 and Fluoresbrite® was probably due to different dissolution properties of these materials in application vehicles and skin: FD-2000 is soluble, but Fluoresbrite® is not. On the other hand, the permeability coefficient of FD-4 (solute diameter 3 nm) through intact skin was around 1×10^{-9} cm/s, similar to the desquamation rate of the upper corneocyte layer. As explained in the theoretical section, chemical materials with $P<1\times10^{-9}$ cm/s did not permeate the stratum corneum under *in vivo* conditions; however, FD-4 permeated not only needle-punctured skin but also razor-treated and stripped skins (Figs. 7, 8). These results suggest that the primary barrier to the skin permeation of FD-4 is permeation of the stratum corneum. It was confirmed that the log *P* of FDs through the skin decreased with an increase in the logarithm of the molecular diameter of FD or log *d* (Fig. 9).

FD-4 was permeated through the intact skin as well as the damaged skin. The cumulative amount of FD-4 permeated through skin over 8 h was in an order of razor-treated>stripped>needle-punctured>intact skin (Fig. 11). The result was similar to the electric resistance, as illustrated in Fig. 10. Fluoresbrite® did not permeate stripped skin or razor-treated skin with low skin electric resistance, but penetrated needle-punctured skin with high skin resistance. In other words, the skin permeation of FDs well correlated with the reciprocal of skin resistance, whereas the skin permeation of Fluoresbrite® did not correlate with the reciprocal of skin resistance (Figs. 12a, b). Other FDs showed a similar tendencies as in FD-4. Therefore, soluble high molecular compounds slightly permeated skin, whereas insoluble nanoparticles did not permeate the viable epidermis or dermis. It is very important to be aware that insoluble nanoparticles may enter porous pathways, such as hair follicles and sweat glands.

CONCLUSION

Nanoparticles, which are considered not to dissolve in dispersion media or skin tissues, permeated only the porous pathway of skin to penetrate into the deep skin. Although they are distributed in the grooves and hair follicles, such insoluble nanoparticles can hardly diffuse in the viable epidermis and dermis. In conclusion, when considering the skin as a dissolution-diffusion membrane, nanoparticles (50 nm in average diameter) do not permeate or penetrate the skin; however, such nanoparticles may permeate a cracked stratum corneum and razor-treated skin. Thus, nanomaterials may affect viable cutaneous cells and, therefore, skin integrity is very important when nanomaterials are applied to the skin.

Acknowledgements This study was supported by a Grant-in-Aid for Scientific Research [H23-iyaku-sitei-016] from the Ministry of Health, Labour, and Welfare, Japan.

REFERENCES

1) Hirose A, Nishimura T, Kanno J. Research strategy for evaluation methods of the manufactured nanomaterials in NIHS and importance of the chronic health effects studies. *Bull. Nat. Inst. Health Sci.*, **127**, 15–25 (2009).
2) German Chemical Industry Association. *Guidance for handling and use of nanomaterials at the workplace 2007.*
3) Steinberg DC. Regulations in chemicals, sunscreen labeling and nanotecnology. *Cosmetic and Toiletries Magazine*, **122**, 36–40 (2007).
4) Wu J, Liu W, Xue C, Zhou S, Lan F, Bi L, Xu H, Yang X, Zeng FD. Toxicity and penetration of TiO_2 nanoparticles in hairless mice and porcine skin after subchronic dermal exposure. *Toxicol. Lett.*, **191**, 1–8 (2009).
5) Schneider M, Stracke F, Hansen S, Schaefer UF. Nanoparticles and their interactions with the dermal barrier. *Dermatoendocrinology*, **1**, 197–206 (2009).
6) Schilling K, Bradford B, Castelli D, Dufour E, Nash JF, Pape W, Schulte S, Tooley I, van den Bosch J, Schellauf F. Human safety review of "nano" titanium dioxide and zinc oxide. *Photochem. Photobiol. Sci.*, **9**, 495–509 (2010).
7) Filipe P, Silva JN, Silva R, Cirne de Castro JL, Marques Gomes M, Alves LC, Santus R, Pinheiro T. Stratum corneum is an effective barrier to TiO_2 and ZnO nanoparticle percutaneous absorption. *Skin Pharmacol. Physiol.*, **22**, 266–275 (2009).
8) Todo H, Kimura E, Yasuno H, Tokudome Y, Hashimoto F, Ikarashi Y, Sugibayashi K. Permeation pathway of macromolecules and nanospheres through skin. *Biol. Pharm. Bull.*, **33**, 1394–1399 (2010).
9) Alvarez-Román R, Naik A, Kalia YN, Guy RH, Fessi H. Skin penetration and distribution of polymeric nanoparticles. *J. Control. Release*, **99**, 53–62 (2004).
10) Sugibayashi K. Margin of safety and exposure of nanomaterials used in cosmetics. *Fragrance Journal*, **36**, 38–41 (2008).
11) Sigma-Aldrich, Co., *Certificate of analysis.*
12) Jyoti KJ, Sabyasachi C, Norma WA, Sanford MS. Synaptotagmin VII Restricts Fusion Pore Expansion during Lysosomal Exocytosis. *PLoS Biol.*, **2**, 1225–1232 (2004).
13) Kraneveld AD, Koster AS, Nijkamp FP. Microvascular permeability in isolated vascularly perfused small intestine of rats. *Am. J. Physiol.*, **266**, G1170–G1178 (1994).
14) Wu X, Price GJ, Guy RH. Disposition of nanoparticles and an associated lipophilic permeant following topical application to the skin. *Mol. Pharm.*, **6**, 1441–1448 (2009).
15) Sekkat N, Kalia YN, Guy RH. Biophysical study of porcine ear skin *in vitro* and its comparison to human skin *in vivo*. *J. Pharm. Sci.*, **91**, 2367–2381 (2002).
16) Simon GA, Maibach HI. The pig as an experimental animal model of percutaneous permeation in man: qualitative and quantitative observations—An overview. *Skin Pharmacol. Appl. Skin Physiol.*, **13**, 229–234 (2000).
17) Zhang W, Gao J, Zhu Q, Zhang M, Ding X, Wang X, Hou X, Fan W, Ding B, Wu X, Wang X, Gao S. Penetration and distribution of PLGA nanoparticles in the human skin treated with microneedles. *Int. J. Pharm.*, **402**, 205–212 (2010).
18) Allec J, Chatelus A, Wagner N. Skin distribution and pharmaceutical aspects of adapalene gel. *J. Am. Acad. Dermatol.*, **36**, S119–S125 (1997).
19) Gamer AO, Leibold E, van Ravenzwaay B. The *in vitro* absorption of microfine zinc oxide and titanium dioxide through porcine skin. *Toxicol. In Vitro*, **20**, 301–307 (2006).
20) Senzui M, Tamura T, Miura K, Ikarashi Y, Watanabe Y, Fujii M. Study on penetration of titanium dioxide (TiO_2) nanoparticles into intact and damaged skin *in vitro*. *J. Toxicol. Sci.*, **35**, 107–113

(2010).
21) Jeong SH, Kim JH, Yi SM, Lee JP, Kim JH, Sohn KH, Park KL, Kim MK, Son SW. Assessment of penetration of quantum dots through *in vitro* and *in vivo* human skin using the human skin equivalent model and the tape stripping method. *Biochem. Biophys. Res. Commun.*, **394**, 612–615 (2010).
22) Lademann J, Richter H, Teichmann A, Otberg N, Blume-Peytavi U, Luengo J, Weiss B, Schaefer UF, Lehr CM, Wepf R, Sterry W. Nanoparticles—An efficient carrier for drug delivery into the hair follicles. *Eur. J. Pharm. Biopharm.*, **66**, 159–164 (2007).
23) Vogt A, Combadiere B, Hadam S, Stieler KM, Lademann J, Schaefer H, Autran B, Sterry W, Blume-Peytavi U. 40 nm, but not 750 or 1500 nm, nanoparticles enter epidermal CD1a+ cells after transcutaneous application on human skin. *J. Invest. Dermatol.*, **126**, 1316–1322 (2006).
24) Toll R, Jacobi U, Richter H, Lademann J, Schaefer H, Blume-Peytavi U. Penetration profile of microspheres in follicular targeting of terminal hair follicles. *J. Invest. Dermatol.*, **123**, 168–176 (2004).

European Journal of Pharmaceutical Sciences 47 (2012) 228–234

Contents lists available at SciVerse ScienceDirect

European Journal of Pharmaceutical Sciences

journal homepage: www.elsevier.com/locate/ejps

In vivo enhancement of transdermal absorption of ketotifen by supersaturation generated by amorphous form of the drug

Kazuhiro Inoue [a,*], Kenji Sugibayashi [b]

[a] *DDS Research Group, Formulation Technology Research Laboratories, Daiichi Sankyo Co., Ltd., 1-2-58 Hiromachi, Shinagawa-ku, Tokyo 140-8710, Japan*
[b] *Faculty of Pharmaceutical Sciences, Josai University, 1-1 Keyakidai, Sakado, Saitama 350-0295, Japan*

ARTICLE INFO

Article history:
Received 13 April 2012
Received in revised form 8 June 2012
Accepted 8 June 2012
Available online 21 June 2012

Keywords:
Ketotifen
Amorphous
Crystalline
Supersaturation
Silicone pressure sensitive adhesive
Transdermal absorption

ABSTRACT

The enhancing effect of supersaturation generated by amorphous ketotifen in silicone pressure-sensitive adhesive matrices (PSA) on the transdermal absorption was evaluated *in vivo* using hairless rats, and it was compared with the increase of drug amount in skin tissues. The duration of the enhancing effect was also investigated in relation to the time how long supersaturation was maintained in PSA. PSA containing crystalline ketotifen (PSA-Crystalline) and that containing amorphous ketotifen (PSA-Amorphous) were prepared by the solvent casting method using n-hexane and dichloromethane, respectively. *In vivo* transdermal absorption was evaluated by measuring the amount of ketotifen in PSAs, the stratum corneum, and viable skin tissues after administration of PSAs on abdominal sites of hairless rats. The amount of ketotifen absorbed into the systemic circulation was calculated by subtracting the drug amount in whole skin tissues from the amount of the drug released from PSAs, then it was monitored for up to 23 h. In both types of PSA, a constant absorption rate was maintained for up to 23 h after 7-h lag time. The enhancement factor of PSA-Amorphous against PSA-Crystalline was approximately 7, which was in good agreement with the difference of drug amount in viable skin tissues. Time course of the drug amount in PSA-Amorphous suggested that the supersaturated level was gradually decreased after 10 h, but the decline of the driving force from PSAs was supplemented by the drug release from the skin depot resulting in the constant absorption rate up to 23 h. These results suggest the usefulness of amorphous ketotifen to obtain enhanced transdermal absorption.

1. Introduction

The drug absorption rate from transdermal drug delivery systems utilizing passive diffusion is proportional to the concentration gradient across the skin, thereby being limited by the drug solubility. Supersaturation is one of the useful tools to overcome this limit (Moser et al., 2001). The efficacy of supersaturation has been proven for piroxicam (Pellet et al., 1994, 1997), fluocinonide (Schwarb et al., 1999) and hydrocortisone (Raghavan et al., 2001) in liquid systems, and for ketoprofen (Kim and Choi, 2002) in adhesive matrix systems. All these supersaturated systems were designed to maintain in a soluble state and some antinucleant agents were incorporated to inhibit the recrystallization. Incorporation of amorphous drug is another approach to obtain a supersaturated system, and it may be superior to the solution system since a constant level of supersaturation can be maintained until the amorphous drug is exhausted from the system. The efficacy of this technique was proven for amorphous ibuprofen prepared by co-milling with kaolin (Mallick et al., 2008). We have been evaluating more convenient methods to generate the amorphous drug in a transdermal adhesive system using ketotifen as a model drug (Inoue et al., 2005).

Ketotifen is the second-generation H1-antihistamine drug. The molecular weight of its free form is 309.1 and the Log *P* is 2.2. The aqueous solubility of crystalline or amorphous ketotifen at 37 °C is 0.052 or 0.438 μmol/cm^3, respectively. Ketotifen is widely used as tablets, capsules, syrups, nasal drops and eye-drops. In addition to these existing dosage forms, the development of transdermal ketotifen is thought to be useful to improve patient compliance and convenience, however it is still an unfulfilled challenge. The current typical dosage regimen is the oral administration of 1 mg twice a day. Our previous study revealed that ketotifen permeates the skin mainly as its free form (Inoue et al., 2000), and the steady-state permeation flux through isolated human stratum corneum from aqueous solution saturated with ketotifen was only 0.4 μg/h/cm^2, suggesting that the native skin permeability of ketotifen will not be sufficient to obtain pharmacological effects by the transdermal route. On the other hand, we found in our preliminary formulation study using silicone pressure-sensitive adhesive matrices (PSA) that ketotifen can be incorporated in PSA as a

* Corresponding author. Tel.: +81 3 3492 3131x4541; fax: +81 3 5436 8568.
E-mail address: inoue.kazuhiro.z8@daiichisankyo.co.jp (K. Inoue).

0928-0987/$ - see front matter © 2012 Elsevier B.V. All rights reserved.
http://dx.doi.org/10.1016/j.ejps.2012.06.006

crystalline or amorphous form depending on the solvent for casting process (Inoue et al., 2005). PSA containing crystalline ketotifen (PSA-Crystalline) was obtained by n-hexane, while amorphous ketotifen was generated in PSA when dichloromethane was used. The PSA containing amorphous ketotifen (PSA-Amorphous) showed a larger skin permeation rate than that of PSA-Crystalline *in vitro*, and the enhanced permeation was maintained for more than 24 h. Since the solubility of amorphous ketotifen is 8.5 times larger than that of crystalline ketotifen (Inoue et al., 2005), we assumed that the concentration of ketotifen in PSA-Amorphous was maintained at a supersaturated level and this caused larger concentration gradient across the skin than the level obtained by PSA-Crystalline.

The first purpose of this study was to confirm if the enhanced transdermal absorption of ketotifen from PSA-Amorphous is observed *in vivo* similarly to the results of previous *in vitro* studies. The second purpose was to check the validity of the assumption that the enhanced *in vivo* skin absorption, if observed, are caused by an increased concentration gradient across the skin by measuring the amount of ketotifen in the skin on which PSA was applied. Here, we considered that the absorption pathway from a transdermal vehicle to blood stream can be divided into two membranes (Mccarley and Bunge, 2001). Our previous study using excised hairless mouse skin revealed that most of the resistance against the permeation of ketotifen resides in the stratum corneum (Inoue et al., 2000). In this study, the amount of ketotifen in the stratum corneum and that in other viable skin tissues were measured separately, and then the correlation between the amount of ketotifen in each compartment and the transdermal absorption rate was evaluated. The third purpose of this study was to evaluate how long the enhanced skin absorption is maintained in an *in vivo* situation by checking the time course of transdermal absorption.

2. Materials and methods

2.1. Materials

Ketotifen fumarate and papaverine hydrochloride (internal standard for HPLC analysis) were purchased from Sigma Chemical Co. (St. Louis, MO, USA). Silicone adhesive PSA (Q7-2920, 50% by wt solution in n-hexane) was provided by Dow Corning Asia Co., Ltd. (Kanagawa, JAPAN). N-hexane and dichloromethane were purchased from Wako Pure Chemical Industries Ltd. (Osaka, JAPAN). Trypsin (type I, isolated from bovine pancreas) was purchased from Sigma Chemical Co. Aluminum laminated film was purchased from Sankyo Seitai Co., Ltd. (Shizuoka, JAPAN) and used as the backing layer. The release liner to protect the adhesive layer was obtained from LINTEC Corporation (Tokyo, Japan). Acetonitrile, triethylamine and acetic acid were purchased from Wako Pure Chemical Industries, Ltd. Male hairless rats, six weeks old, were purchased from Charles River Laboratories Japan, Inc. (Kanagawa, Japan) for both *in vivo* studies and for collection of skin samples for *in vitro* permeation studies.

2.2. Methods

2.2.1. Preparation of PSA

PSA-Crystalline and PSA-Amorphous were prepared according to the previous procedure (Inoue et al., 2005). Ketotifen free base was precipitated from aqueous solution of ketotifen fumarate by alkalization followed by washing with purified water and drying *in vacuo*. The ketotifen thus obtained has been confirmed to be amorphous by its X-ray diffraction pattern and differential scanning calorimetry profile (Inoue et al., 2005). The amorphous ketotifen was dispersed in n-hexane to obtain supersaturated solution, from which crystalline ketotifen was precipitated under vigorous agitation. The suspension of crystalline ketotifen thus obtained was mixed with PSA polymer solution, then the mixture was coated and dried on the backing film by a coating machine (Test Coater, Yasui Seiki, Tokyo, Japan) to get PSA-Crystalline. In the case of PSA containing amorphous ketotifen, the free base was dissolved in dichloromethane and it was mixed with PSA polymer solution followed by coating and drying. The amount of raw materials to prepare the two types of PSA were summarized in Table 1. After drying, PSA was covered by a release liner film, then cut into circular pieces having diameter of 1.4 cm or 2.0 cm, respectively for *in vitro* or *in vivo* study.

The amount of ketotifen in a piece of PSA was determined by dissolving a piece in 5 mL of n-hexane followed by extracting the ketotifen into 3 mL acidic aqueous phase (0.01 N HCl). The aqueous phase was assayed by HPLC with the absolute calibration curve method, then the ketotifen amount in PSA was calculated by multiplying the ketotifen concentration with the volume of the aqueous phase (3 mL). The ketotifen amount was divided by the area of the adhesive face to obtain the drug amount per unit area. The measurement was repeated 10 times and the mean value was defined as the initial amount of ketotifen in PSA.

2.2.2. In vivo study

Two sets of *in vivo* experiment were conducted. In both experiments, all animal handling procedures were in accordance with the guidelines of the Institutional Animal Care and Use Committee of Daiichi Sankyo Co., Ltd.

2.2.2.1. Time course of ketotifen amount in PSA, the stratum corneum and viable skin tissues during the administration. Eighteen hairless rats were divided into two groups. Ten rats were assigned for the test group of PSA-Crystalline, and others were assigned for PSA-Amorphous. Animals were anesthetized with ether, the abdominal skin was cleaned with absorbent cotton, then two PSAs were administered on the abdominal site with 2-cm distance between pieces. After the administration, surgical tape (Elatex®, Alcare Co., Ltd.) was put around the trunk of the animals for protection of PSAs, then each animal was kept separately in a cage and allowed free access to water until the sampling time. At each sampling time, an animal was euthanized by carbon dioxide, then two pieces of silicone PSAs were gently peeled off. The stratum corneum on the administration sites was collected by tape-stripping with adhesive tape (Cellotape®, Nichiban Co., Ltd.) 20 times followed by the excision of underlying viable skin tissues. The sampling time was 2, 4, 6, 8, 10, 13, 15, 17, 20, and 23 h for the PSA-Crystalline group, and 2, 4, 7, 10, 13, 16, 19, and 23 h for the PSA-Amorphous group. From one administration site, one set of samples consisting of one PSA, 20 tape-stripped stratum corneum samples, and a piece of viable skin tissues, was obtained. At each sampling time, two sets of samples were obtained from one animal. In a preliminary experiment, it has been confirmed that no ketotifen was detected in the stratum corneum from which PSA was removed immediately

Table 1
The amount of raw materials to prepare silicone pressure-sensitive adhesive matrices containing ketotifen.

	PSA-Crystalline	PSA-Amorphous
Ketotifen (g)[a]	0.250	0.594
Silicone PSA (g)[b]	15.04	15.03
N-hexane (g)	5.74	–
Dichloromethane (g)	–	6.21

[a] Free base.
[b] 50%(w/w) solution in n-hexane.

after the administration, suggesting that PSA can be completely removed from the stratum corneum with this procedure.

The amount of ketotifen in PSA was determined according to the same procedure in Section 2.2.1., and the decrease in the amount from the initial value was defined as the drug release. The ketotifen amount in the stratum corneum and viable skin tissues were determined according to the procedures described in Sections 2.2.5 and 2.2.6. The amount of ketotifen absorbed into the systemic circulation was calculated by subtracting the sum of the ketotifen amount in the stratum corneum and in the skin from the drug amount released (Calculated Transdermal Absorption).

2.2.2.2. Time course of ketotifen amount in the stratum corneum and viable skin tissues after the removal of PSA. Six rats were anesthetized with ether, the abdominal skin was cleaned with absorbent cotton, then two pieces of PSA-Crystalline were administered on the abdominal site with 2-cm distance between pieces. The PSAs were protected by surgical tape, and each animal was isolated in a cage and allowed free access to water. Four hours after the administration, all animals were anesthetized with ether, then all PSAs were removed. One animal was immediately euthanized by carbon dioxide, then the stratum corneum and underlying skin tissues on the administration sites were collected according to the procedures in the previous section. Other five animals were further kept in individual cages until the sampling time for 3, 6, 13, 18, or 23 h followed by the sampling of the stratum corneum and the viable skin tissues after euthanasia with carbon dioxide. From one administration site, one set of samples consisting of 20 tape-stripped stratum corneum samples and viable skin tissue was obtained. At each sampling time, two sets of samples were obtained from one animal.

The amount of ketotifen in silicone PSA was determined according to the same procedure in Section 2.2.1., and the decrease in the ketotifen amount from the initial value was calculated as the drug release. The ketotifen amount in the stratum corneum and in the viable skin tissues were determined according to the procedures described in Sections 2.2.4 and 2.2.5.

2.2.3. In vitro study

The estimation of *in vivo* transdermal drug absorption noted above was based on the assumption that the drug release from PSA subtracted with the drug amount in the whole skin represents the amount of ketotifen absorbed into the systemic circulation. In order to confirm the validity of this assumption, the drug release from the PSA subtracted with the drug amount in the skin was compared with the actual permeation in the following *in vitro* studies. Some abdominal full-thickness skin samples were excised from hairless rats and stored at −60 °C until use. The frozen skin samples were slowly thawed at room temperature, cut into pieces, and mounted on a vertical Franz-type diffusion cells with 1.77-cm^2 effective permeation area and 12-mL capacity of the receptor chamber. Isotonic phosphate-buffered saline (pH 7.4) containing 0.1%(w/w) of sodium azide (receptor buffer) was filled in the receptor chamber, and the temperature was kept at 37 °C by isothermal water circulator. Twenty-four cells were divided into two groups. Twelve cells were assigned for the PSA-Crystalline group and others were assigned for PSA-Amorphous. A piece of PSA was put on the skin, and the cell was incubated until the sampling time. At the sampling time, the PSA was gently peeled off the skin and the receptor buffer was collected from the receptor chamber, then the stratum corneum was collected by tape-stripping with adhesive tape 20 times. The sampling time was 4, 8, 14, 17, 20, and 24 h for both the PSA-Crystalline group and PSA-Amorphous group. At each sampling time, samples were obtained from two cells.

The concentration of ketotifen in the receptor buffer was assayed by HPLC according to the procedure in Section 2.2.6 with the absolute calibration curve method. The amount of ketotifen in PSAs was determined according to the same procedure in Section 2.2.1, and the decrease in the amount from the initial value was calculated as the drug release. The ketotifen amount in the stratum corneum and in the viable skin tissues were determined according to the procedures described in Sections 2.2.4 and 2.2.5. In this experiment, the amount of ketotifen permeated through the skin was directly obtained by multiplying the concentration of ketotifen in the receptor buffer with the receptor volume (12 mL) (Actual Skin Permeation), or indirectly obtained by subtracting the sum of the ketotifen amount in the stratum corneum and in the skin from the drug release (Calculated Skin Permeation). Actual Skin Permeation and Calculated Skin Permeation were compared to check the validity of the procedure to estimate *in vivo* absorption described in 2.2.2.1.

2.2.4. Amount of ketotifen in the stratum corneum

The 20 tape-stripped stratum corneum samples were soaked in 5 mL of n-hexane, and 3 mL of aqueous solution containing 0.01 N HCl was added to the organic phase followed by agitation for 2 min by a vortex mixer. The organic phase and the aqueous phase were separated by centrifugation (3000 rpm, 10 min), then the concentration of ketotifen in the aqueous phase was obtained by HPLC with the absolute calibration curve method. The amount of ketotifen in the stratum corneum was calculated by multiplying the concentration of ketotifen with the volume of the aqueous phase (3 mL), then it was divided by the area of PSA. In a preliminary experiment, it has been confirmed that more than 95% of ketotifen was recovered in this procedure.

2.2.5. Amount of ketotifen in viable skin tissues

A viable skin tissue sample was cut into small pieces, and incubated in 2 mL of phosphate buffered saline (pH 7.4) containing 50 μg/mL papaverine hydrochloride as the internal standard and 0.2%(w/v) trypsin as the digestant at 37 °C overnight. After the incubation, 3 mL of aqueous solution containing 1 N NaOH and 5 mL of n-hexane were added and they were vigorously agitated by a vortex mixer for 2 min. After the agitation, the organic phase was separated by centrifugation (3000 rpm, 10 min) from the aqueous phase, and was transferred into another tube. The organic phase was then mixed with 3 mL of aqueous solution containing 0.01 N HCl followed by centrifugation (3000 rpm, 10 min). The aqueous phase thus obtained was analyzed by HPLC, and the ratio of the peak area of ketotifen to that of papaverin was calculated. The amount of ketotifen in the viable skin tissues was calculated by substituting the area ratio into the standard curve prepared by the same procedure described above with skin samples containing known amount of ketotifen, then it was divided by the area of PSA.

2.2.6. HPLC condition

The HPLC analysis was performed using an HPLC system (LC-10, Shimadzu, Kyoto, Japan) equipped with an ODS column (A-312, YMC, Kyoto, Japan). The temperature of the column was maintained at 40 °C. The mobile phase was acetonitrile/water/triethylamine/acetic acid (500/500/2/1 in volume ratio), and the flow rate was 1.0 mL/min. Ketotifen and papaverin were detected by ultraviolet absorbance at 312 nm.

2.2.7. Calculation of in vivo transdermal absorption rate and in vitro skin permeation rate

Using the data sets in the linear portion of the transdermal absorption profile *in vivo* or in the skin permeation profile *in vitro*, the absorption rate or the permeation rate was calculated